Investigation of Microstructures of AlAs Oxides Before and After Oxidation *

WANG Yong(王勇)[1], JIA Hai-Qiang(贾海强)[1], MAI Zhen-Hong(麦振洪)[1**],
JIA Quan-Jie(贾全杰)[2], JIANG Xiao-Ming(姜晓明)[2]

[1]*Institute of Physics, Chinese Academy of Sciences, Beijing 100080*
[2]*Institute of High Energy Physics, Beijing Synchrotron Radiation Facility, Beijing 100039*

(Received 10 March 2004)

The effect of lateral oxidation on microstructures of the GaAs/AlAs/GaAs heterostructure was studied by x-ray specular reflectivity, nonspecular scattering and diffraction. The GaAs/Al_2O_3/GaAs multilayer was obtained after oxidation of the GaAs/AlAs/GaAs sample. The results show that, before oxidation, there are two 40-Å-thick intermixing layers, one located between the AlAs sublayer and the GaAs substrate, and the other between the AlAs sublayer and the upper GaAs sublayer. After oxidation, these two intermixing sublayers disappear. The AlAs was oxidized into amorphous Al_2O_3 totally. The surface and interface roughnesses of the sample also decrease after oxidation.

PACS: 73. 40. Ty, 61. 10. Nz, 61. 10. Eq

Recently, native oxides of AlAs alloys [1] have attracted great interest due to their applications in distributed Bragg reflectors (DBRs) of vertical-cavity surface-emitting lasers (VCSELs).[2,3] Dielectric apertures formed in this native oxide layer have dramatically improved optical and current confinements and have enabled ultra-low threshold currents and high output power efficiencies.[4] AlAs oxides have also found many other applications, for example as insulating layers in metal-oxide–semiconductor field effect transistors,[5,6] current guiding layers in heterojunction bipolar transistors,[7] and insulating buffer layers for metal–semiconductor field-effect transistors.[8] The oxides are usually formed by direct wet thermal oxidization of AlAs into Al_2O_3 during postgrowth processing.[9] Great efforts have been taken to have the optical and electronic properties improved by AlAs oxide. However, the microstructure of the AlAs oxide is not understood clearly. The oxidation degree of AlAs and the roughness of surface and interface both significantly influence the quality of the AlAs oxide. In this Letter, we study the microstructures of the GaAs/AlAs/GaAs heterostructure before and after lateral oxidation by x-ray specular reflectivity, nonspecular scattering and diffraction. The results show that the lateral oxidation can strongly affect the microstructures of GaAs/AlAs/GaAs.

Epilayers were grown in a V80H molecular-beam epitaxy system at 580°C. The nominal structure of the samples was GaAs/$In_xAl_{1-x}As$(50 Å)/AlAs(1000 Å)/$In_xAl_{1-x}As$(50 Å)/GaAs(500 Å). The $In_xAl_{1-x}As$ was used as a surfactant. The content of In was extremely low. The deposition speeds of GaAs and AlAs were 1 μm/h and 0.2 μm/h, respectively. Because of the protection of GaAs from oxidation, the lateral oxidation approach was used. Firstly, 3-μm-wide grooves deepening to the substrate was corroded on the sample surface by a hot-etching technique. The interval of the grooves was 50 μm as shown in Fig. 1. One sample was then put into a tubular equipment with de-ionized water at 80°C and oxidized at 450°C for 40 min. The oxidation proceeds laterally into the sample from the grooves. The as-deposited one is sample 1 in the following discussion and the oxidized sample is referenced as sample 2.

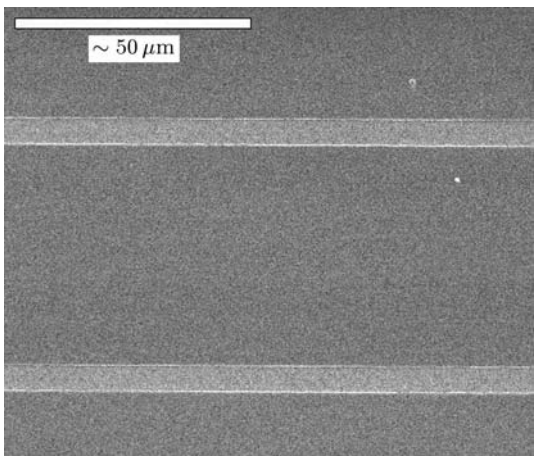


Fig. 1. SEM photograph of the sample surface.

X-ray specular reflectivity and nonspecular scattering measurements were performed at the x-ray diffuse scattering station at beam line 4W1C of the Beijing Synchrotron Radiation Facility (BSRF). The photon energy was selected at the $K_{\alpha 1}$ characteristic x-radiation of Cu, 8.050 keV. The incidence plane was parallel to the grooves. Both the incidence beam and detector slits were 0.2 mm.

Figure 2(a) shows the x-ray specular reflectivity (open circles) and the theoretical simulation (solid lines) of sample 1, the as-deposited sample. The theoretical simulation followed the Paratt formulism.[10,11] The best fitting parameters are listed in Table 1. It

* Supported by the National Natural Science Foundation of China under Grant No 10274096.
** To whom correspondence should be addressed. Email: zhmai@aphy.iphy.ac.cn
©2004 Chinese Physical Society and IOP Publishing Ltd

can be seen from Table 1 that there are two 40 Å-thick intermixing layers inside sample 1, one located between the AlAs layer and the substrate, the other between the AlAs layer and the upper GaAs layer. In our calculation, it was assumed that the composition and the density of the intermixing layer vary linearly from the bottom to the top. In other words, the composition of the intermixing layer is $Al_yGa_{1-y}As$, in which the value of y varies linearly from 0 to 1 as a function of the vertical position of the sample. Figure 2(b) shows the simulation result with the intermixing layers replaced by an $Al_{0.5}Ga_{0.5}As$ layer of the same thickness. Comparing Figs. 2(a) and (b), one can see that the simulated curve considering y as linear variation are better than that with $y = 0.5$. Because there are two 50-Å-thick $In_xAl_{1-x}As$ surfactant layers deposited above and below the AlAs layer, it can be reasonably assumed that the existence of intermixing layers is due to the $In_xAl_{1-x}As$ surfactant layers.

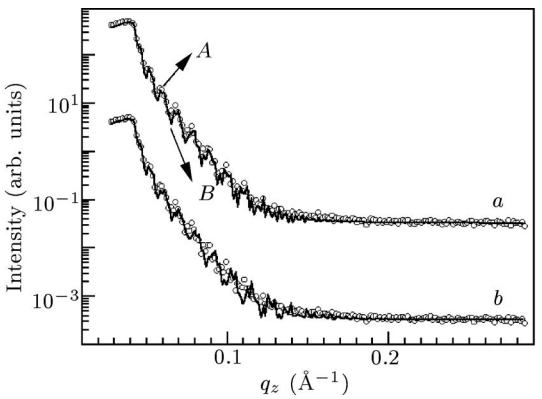


Fig. 2. X-ray reflectivity and simulated curves of sample 1. The open circles represent the experimental data and the solid lines are the fittings. (*a*) The best fitting and (*b*) the fitting considering $Al_{0.5}Ga_{0.5}As$ instead of continuous intermixing layer between AlAs and GaAs sublayers. A and B mark the position of q_z at which the diffuse scattering measurements were performed.

Figure 3 is the measured and simulated reflectivity profile for sample 2. The simulated parameters are also listed in Table 1. It can be seen from Fig. 3 that after oxidation, the AlAs layer was oxidized into Al_2O_3. The two intermixing layers shown in sample 1 disappear. The roughnesses of the surface and interface of sample 2 decrease, compared to that of sample 1. The total content of Al in the AlAs and the two intermixing layers or/and in the Al_2O_3 layer are $0.0129\,mg/cm^2$ and/or $0.0122\,mg/cm^2$ for samples 1 and 2, respectively. This means that the content of Al in the two samples is almost the same. X-ray high angle diffractions were performed. The result is illustrated in Fig. 4. It is obvious from Fig. 4 that there is a sharp peak of the AlAs layer in curve *a*. This means that the AlAs layer was a good epitaxial layer before oxidation. There is only a sharp peak of GaAs in curve *b*, showing that after oxidation, AlAs was oxidized into Al_2O_3 totally and the Al_2O_3 layer was in an amorphous state, which is in agreement with the results of Yoshikawa *et al.*[12] Because the oxidizing temperature is 450°C, the oxidation process was also an annealing one. The free energy of the interface would decrease after the annealing. For the interface between crystal and amorphous films, smaller roughness will introduce a smaller free energy; therefore the roughness of the interface will decrease after oxidation.

Table 1. Simulated structure parameters for the x-ray reflectivity of the samples. The roughness of every row represents the roughness at the interface between the corresponding layer and the upper layer.

	Layer	Density (g/cm^3)	Thickness (Å)	Roughness (Å)
Sample 1	GaAs	5.32 ± 0.01	500 ± 1	18 ± 1
	Intermixing layer		40 ± 1	10 ± 1
	AlAs	3.73 ± 0.01	1300 ± 10	15 ± 1
	Intermixing layer		40 ± 1	9 ± 1
	GaAs substrate	5.32 ± 0.01		5 ± 1
Sample 2	GaAs	5.32 ± 0.01	505 ± 1	8 ± 1
	Al_2O_3	1.78 ± 0.01	1300 ± 10	10 ± 1
	GaAs substrate	5.32 ± 0.01		5 ± 1

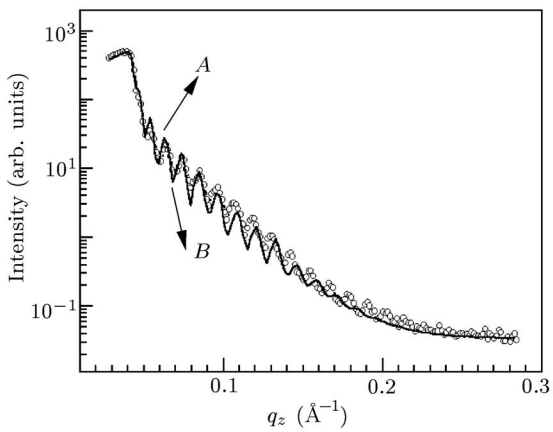


Fig. 3. X-ray reflectivity and simulated curves of sample 2. The open circles represent the experimental data and the solid lines are the fitting ones. *A* and *B* mark the position of q_z at which the diffuse scattering measurements were performed.

As is well known, specular scans perpendicular to the interfaces of the sample do not provide the lateral interfacial information. For investigating the lateral interfacial structure, nonspecular scattering was measured. The description of the experimental setup has been reported by Stettner *et al.*[13] The theoretical method for analysis of nonspecular scattering from the layered system within the distorted-wave Born approximation (DWBA) has been developed by Holy and co-workers [14,15] and other researchers.[16] The roughness obtained from the theoretical simulation of the x-ray reflectivity is the total roughness, including the correlated and the uncorrelated ones. The roughness referenced in the expression of correlation function is correlated roughness, which can be obtained from the simulation of nonspecular scattering profile. The relation between them is $\sigma^2_{\text{total}} = \sigma^2_{\text{cor}} + \sigma^2_{\text{uncor}}$.[17]

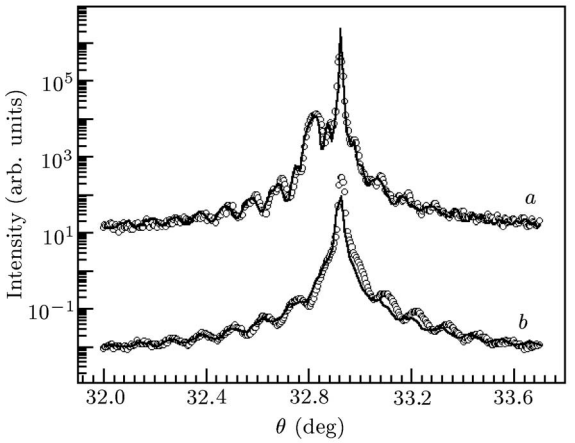


Fig. 4. X-ray high angle diffraction curves of (a) sample 1 and (b) sample 2. The open circles represent the experimental data and the solid lines are the fittings.

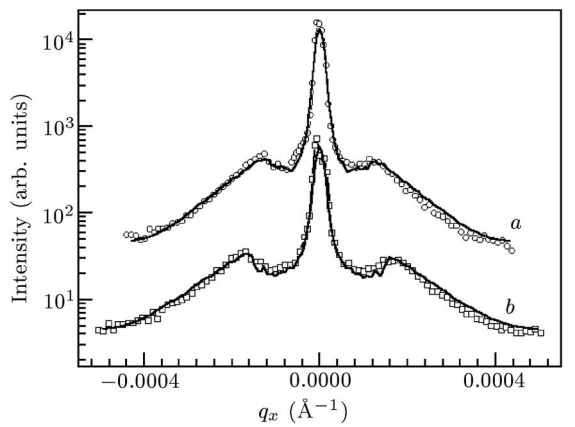


Fig. 5. X-ray transverse diffuse scattering curves for sample 1. The solid line is the fitting to the diffuse scattering data represented by circles. The q_z values at which the transverse scans were performed are 0.05976 Å^{-1} and 0.06544 Å^{-1}, respectively (see the marks in Fig. 2).

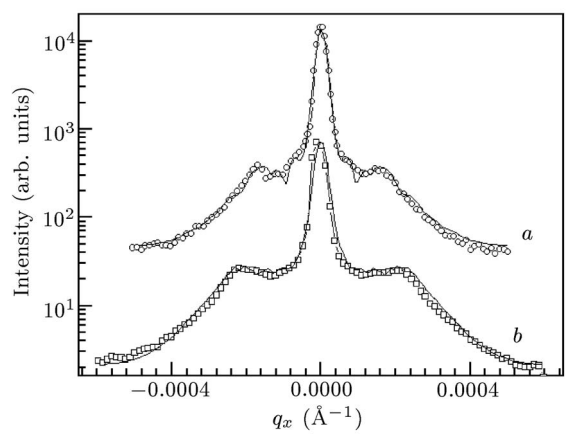


Fig. 6. X-ray nonspecular scattering curves for sample 2. The solid line is the fitting to the reflectivity represented by circles. The values of q_z for curves a and b are 0.06409 Å^{-1} and 0.06836 Å^{-1}, respectively, marked in Fig. 3.

Figures 5 and 6 show the nonspecular scattering curves of samples 1 and 2, respectively. Curves a and b in the figures represent the nonspecular scattering measured at points marked by A and B in Fig. 2 and 3, respectively. The simulated parameters are listed in Table 2. It can be seen from Table 2 that the fractal exponent h of sample 2 is lower than that of sample 1, showing that the interfaces of sample 2 becomes more jagged after oxidation. Because the AlAs has been oxidized into Al_2O_3, the epitaxial structure of the AlAs sublayer was destroyed after oxidation. Therefore, the vertical correlation length decreases from 10000 Å to 1000 Å. Meanwhile, the correlated roughness and the horizontal correlation length decrease, indicating that the fluctuation of the surface and interface of sample 2 become smaller and more abrupt after oxidation.

Table 2. Simulated parameters of the x-ray diffuse scattering of the samples.

Sample	h	$\xi_{\parallel}$ (Å)	$\xi_{\perp}$ (Å)	$\sigma_{\rm cor}$ (Å)
1	0.8 ± 0.1	1000 ± 10	10000 ± 10	5 ± 1
2	0.2 ± 0.1	300 ± 10	1000 ± 10	3 ± 1

In summary, we have investigated the effect of lateral oxidation on the microstructures of GaAs/AlAs/GaAs. The results show that before oxidation, two 40-Å-thick intermixing layers exist inside the sample, one located between the AlAs layer and the substrate, the other between the AlAs layer and the upper GaAs layer. After oxidation, the AlAs sublayer was oxidized into Al_2O_3 and the Al_2O_3 sublayer is of an amorphous state. The two intermixing layers which existed before oxidation disappear and the surface and interface roughnesses of the oxidized sample decrease. The results from the nonspecular scattering show that the fluctuation of surface and each interface become more abrupt after oxidation. Compared to that of the non-oxidized sample, this means that lateral oxidation is an effective method to prepare AlAs oxide.

References

[1] Dallesasse J M et al 1990 *Appl. Phys. Lett.* **57** 2844
[2] Huang Z C and Wu H Z 2004 *Chin. Phys. Lett.* **21** 316
[3] Wierer J J et al 1997 *Appl. Phys. Lett.* **71** 2286
[4] Huffaker D L et al 1994 *Appl. Phys. Lett.* **65** 97
[5] Lin Q et al 2003 *Chin. Phys. Lett.* **20** 158
[6] Zhu M et al 2003 *Chin. Phys. Lett.* **20** 767
[7] Zhou J and Zhang G Y 2002 *Chin. Phys. Lett.* **19** 707
[8] Li X J et al 2001 *Chin. Phys. Lett.* **18** 1147
[9] Huffaker D L et al 1994 *Electron. Lett.* **30** 1946
[10] Paratt L G 1954 *Phys. Rev.* **95** 359
[11] Born M and Wolf E 1964 *Principles of Optics* 2nd edn (Oxford: Pergamon)
[12] Yoshikawa T et al 1998 *Appl. Phys. Lett.* **72** 2310
[13] Stettner J et al 1996 *Phys. Rev.* B **53** 1398
[14] Holy V and Baumbach T 1994 *Phys. Rev.* B **49** 10668
[15] Holy V et al 1993 *Phys. Rev.* B **47** 15896
[16] Schlomka J P et al 1995 *Phys. Rev.* B **51** 2311
[17] Savage D E et al 1991 *J. Appl. Phys.* **69** 1411